

Supporting Information

Fishman et al. 10.1073/pnas.1213228110

SI Materials and Methods

Scaffold Preparation and Characterization. Tissue was harvested and scaffolds prepared as described (1, 2). Larynges were removed from adult donor rabbits (New Zealand White) from unrelated studies, following euthanasia by anesthetic overdose. All surgical procedures and animal handling were performed in accordance with The Animals (Scientific Procedures) Act 1986 and Home Office Codes of Practice (Home Office personal licence: PIL 70/23493, J.M.F.) and under relevant ethical approval. The cricoarytenoid dorsalis (CAD) muscle was dissected from each larynx and either used fresh or decellularized.

For decellularization, a nondetergent, nonproteolytic protocol was used that preserves the major components of the extracellular matrix (ECM) (1, 2). Muscles were incubated in 50 nM latrunculin B (Sigma-Aldrich) in high-glucose DMEM (DMEM; Gibco) for 2 h at 37 °C to depolymerize actin filaments. All further steps were performed at room temperature. CAD muscles were washed with distilled water twice for 15 min between incubation steps, resulting in cell lysis by osmotic shock. After incubation in latrunculin B, muscles were incubated in 0.6 M potassium chloride (KCl) (Sigma-Aldrich) for 2 h, followed by 1.0 M potassium iodide (KI) (Sigma-Aldrich) for 2 h according to ref. 3. Exposure to these high ionic strength salt solutions results in depolymerization of myosin filaments. Following the salt solution incubations, muscles were washed in distilled water overnight and then the potassium chloride and potassium iodide incubations were repeated, followed by incubation in 1 KU/mL DNase I (Sigma-Aldrich) in PBS for 2 h to digest DNA. Finally, treated muscles were washed in distilled water for a minimum of 2 d with daily water changes to remove remaining reagents and residual DNA.

DNA was extracted and quantified within fresh tissue and decellularized scaffolds, respectively, by using the GenElute Mammalian Genomic DNA Miniprep Kit (Sigma-Aldrich). Collagen and sulfated-glycosaminoglycans were quantified by using the Sircol Collagen and Blyscan Glycosaminoglycan Assay Kits respectively (Biocolor).

Histology and Immunohistochemistry. Samples were fixed for 24 h in 10% neutral buffered formalin (NBF) solution in PBS (pH 7.4) at room temperature. Subsequently, they were washed in distilled water, dehydrated in graded alcohol, embedded in paraffin, and sectioned at 5 μ m. Tissue slides were stained with hematoxylin and eosin (H&E) (Leica Biosystems UK and Pioneer Research Chemicals), Picro-sirius red (Sigma-Aldrich and BDH Laboratory Supplies), Miller's elastin (Pioneer Research Chemicals), and Alcian blue [1% (wt/vol) Alcian blue in 3% (vol/vol) acetic acid at a pH of 2.5 for 30 min] (Leica). Slides were visualized with an Olympus BX40 light microscope, and images were captured with Olympus DP Controller software (Olympus Optical, version 1.1).

For the immunohistochemical analysis, paraffin sections were cut and mounted on to 2% (3-aminopropyl)triethoxysilane (Sigma-Aldrich) coated slides. Sections were incubated with monoclonal antibody to Myosin Heavy Chain (Sigma-Aldrich), MHC class II (VMRD), CD68 (AbD Serotec), CCR7 (Epitomics), CD163 (Hycult Biotech), CD86, Arginase I, CD3, CD4, FoxP3 (all Abcam), Alpha Smooth Muscle Actin (Sigma-Aldrich), and Factor VIII (Biocare Medical) according to standard immunohistochemical protocols by using an avidin-biotin-based detection system (Vector Laboratories).

For immunohistochemistry on fresh-frozen samples, specimens were embedded in optimal cutting temperature compound

(Tissue-Tek; Sakura Finetek UK) and snap-frozen in isopentane (2-methylbutane; Sigma-Aldrich) precooled over liquid nitrogen. Five-micrometer sections were cryosectioned on a Leica CM3000 cryostat (Leica) and incubated with the monoclonal antibodies to MHC class I (AbD Serotec), EYFP (Invitrogen), CD163 (AbD Serotec), and FoxP3 (Abcam).

Transmission Electron Microscopy. Samples were fixed immediately after harvesting (to prevent degradation) in 4% (vol/vol) glutaraldehyde (Agar Scientific) in 0.1 M phosphate buffer and left for 24 h at 4 °C. After washing in 0.1 M phosphate buffer (pH 7.4), samples were fixed in 1% OSO4/0.1 M phosphate buffer (pH 7.3) at 4 °C for 1.5 h and then washed again in 0.1 M phosphate buffer (pH 7.4). Specimens were stained en bloc with 0.5% uranyl acetate in distilled water (dH₂O) at 4 °C for 30 min, rinsed with dH₂O, dehydrated in a graded ethanol-water series and infiltrated with Agar 100 resin and then hardened. Sections measuring 1 μ m were cut and stained with 1% toluidine blue in distilled water for light microscopy. A representative area was selected and sections were cut at 70–80 nm by using a diamond knife on a Reichert ultra-cut E microtome. Sections were collected on a 200-mesh copper, coated slot grid and stained with uranyl acetate and lead citrate. Images were recorded with a Joel 1010 transmission electron microscope and captured with a Gatan digital camera.

Scanning Electron Microscopy. Samples were fixed, immediately after harvesting, in 4% (vol/vol) glutaraldehyde (Agar Scientific) in 0.1 M phosphate buffer and left for 24 h at 4 °C. Following washing with 0.1 M phosphate buffer, the specimens were cryoprotected in 25% sucrose, 10% glycerol in PBS (pH 7.4) for 2 h, then fast frozen in liquid nitrogen slush and fractured at approximately –160 °C. Samples were then placed back into cryoprotectant at room temperature and allowed to thaw. After washing in 0.1 M phosphate buffer (pH 7.4), the material was fixed in 1% OSO4/0.1 M phosphate buffer (pH 7.3) at 4 °C for 1.5 h and washed again in 0.1 M phosphate buffer (pH 7.4). After rinsing with dH₂O, specimens were dehydrated in a graded ethanol-water series to 100% ethanol, critical point dried by using CO₂, and finally mounted on aluminum stubs by using sticky carbon tabs. The fractured material was mounted to present fractured surfaces to the beam and then coated with a thin layer of Au/Pd (~2 nm thick) by using a Gatan ion beam coater. Images were recorded with a Jeol 7401F field emission scanning electron microscope and captured with Jeol software.

Biomechanical Assessment. Biomechanical characteristics of native and decellularized muscle were evaluated by uniaxial tensile stress testing. Excised samples, of comparable dimensions, were analyzed fresh and stored in PBS at 4 °C until evaluation. All of the measurements were carried out directly after withdrawal out of PBS under constant ambient conditions (20 \pm 1 °C). Samples were continuously wetted with PBS throughout testing to prevent dehydration. Samples were tested to rupture, starting with an initially applied uniaxial tensile load of 1 mN and increasing at a rate of 200 mN/min up to a maximum force of 6 N, or until rupture (whichever occurred first) by using a Dynamic Mechanical Analyzer Instrument (DMA 7e; PerkinElmer) and Pyris software, version 6.0 (PerkinElmer). The tensile tester recorded the load and elongation to which the tissue was subjected in real time.

Engineering stress, σ , was defined as the tensile force divided by the original cross-sectional area (thickness and width of each specimen were measured by digital calipers at three different

positions before testing and averaged), whereas the strain, ϵ , was defined as the ratio between the grip displacement and the initial gripping distance (as measured by using digital calipers at three different positions and averaged). The maximum tangential tensile Young's modulus, E , was defined as the maximum slope of the stress-strain curve in the linear region (i.e., maximum resistance to deformation), expressed in kilopascals. Rupture force was defined as the maximum force that a test specimen can support during a tensile test of loading to break, expressed in millinewtons. Tensile strength was defined as the rupture load or force per unit of cross-sectional area of the unstrained specimen, expressed as kilopascals. Elongation at break (tissue deformation) was defined as the increase in length of a test specimen that results from subjecting it to the rupture force in a tensile test, expressed as a percentage of the initial length. Six samples were considered for each evaluated tissue.

Chicken Egg Chorioallantoic Membrane Assay. To evaluate the angiogenic properties of the decellularized tissue, we used the chicken egg chorioallantoic membrane (CAM) assay, as described (4–6). Fertilized chicken eggs (Henry Stewart and Co.) were incubated at 37 °C and constant humidity. After 3 d of incubation, an oval window of ~3 cm in diameter was cut into the shell with small dissecting scissors to reveal the embryo and CAM vessels. The window was sealed with tape, and the eggs returned to the incubator for a further 5 d. At day 8 of incubation, 1-mm diameter decellularized scaffolds, fresh tissue, or gelatin sponges (Spongostan; Ethicon) soaked in either PBS (negative control), or 400 ng/mL human recombinant VEGF-165 (positive control; Biologend) were placed on the CAM between branches of blood vessels. Samples were examined daily until 6 d after placement wherein they were photographed *in ovo* with a stereomicroscope equipped with a Camera System (Leica MZ FL111) to quantify the blood vessels surrounding the implants. The number of blood vessels less than 10 μm in diameter converging toward the placed tissues was counted blindly by assessors ($n = 38$ eggs), with the mean of the counts being considered.

Biocompatibility Study. For the 2-, 4- and 8-wk biocompatibility studies, 24 adult male Sprague–Dawley rats (Harlan Laboratories), weighing 250–380 g were anesthetized by using 0.25 mL of intramuscular Hypnorm (0.315 mg/mL fentanyl citrate and 10 mg/mL fluanisone) and 1 mg of i.p. diazepam. Before implantation and immediately preoperatively, specimens were sterilized with ultraviolet light treatment (30 min each side). A midline incision was made through the shaved skin on the abdomen. Fresh and/or decellularized rabbit muscles were implanted under aseptic technique into s.c. pockets formed on the right and left side of the midline incision. Each sample was held in place by using a single 4/0 Prolene suture (Ethicon, Johnson & Johnson Medical). Skin was closed with 3/0 Mersilk sutures (Ethicon). Rats were weighed immediately preoperatively and before euthanasia. Rats were euthanized at the relevant time-points by anesthetic overdose (lethal dose of sodium pentobarbitone by i.p. injection, 200 mg/mL), at which point the explants were harvested and processed.

Quantitative Histology and Immunohistochemistry. Three-dimensional quantitative stereological techniques were used to quantify scaffold volume (for biodegradation studies), the host immune response toward the scaffold *in vivo*, and vascularization. All scaffolds were prepared according to the requirements of stereological techniques. Following fixation, the length of each postimplantation scaffold was measured in millimeters and sliced into ~4 sections (n) of roughly equal thickness (t) in preparation for total volume estimation and subsequently paraffin wax embedded. Following routine hematoxylin/eosin staining on 5- μm sections, the total volume of each scaffold (V_{ref}) was estimated by using Cavalieri's principle (7). Using a microfiche, a grid of quadratically arranged test points

was randomly superimposed onto the cut surface of each scaffold slice, and the number of points overlying the scaffold/tissue area was counted. V_{ref} was then estimated by multiplying the total number of points for all slices by the area associated with each point (A_p) and the mean section thickness (t).

The volume fraction of blood vessels (V_V) within each scaffold for each implantation period was estimated by using the unbiased stereological technique of point counting using a quadratic array of test points as described (8). Blood vessels were identified via immunolocalization with the endothelial cell marker, Factor VIII. All stereological estimations were aided by Visiopharm Integrator System (Visiopharm) and Kinetic Imaging Stereology Software, version 5.0 (Kinetic Imaging) at a final magnification of 40 \times and ~40 fields of view were analyzed for each scaffold. Briefly, a digital grid of quadratically arranged test points was randomly superimposed onto the surface of each imaged scaffold section, and the numbers of test points overlying blood vessels were counted for each uniformly random selected field of view. The sum of all points hitting the blood vessels was divided by the sum of all points hitting the area of interest over all fields analyzed, generating a volume fraction of the tissue occupied by blood vessels (V_V). The volume fraction was considered the main scaffold-related parameter characterizing the extent of neovascularization (reflecting both the number and size of new blood vessels).

Twenty-five-micrometer immunolabeled sections were used to obtain the numerical density of CD3, CD4, FoxP3, CD68, CCR7, CD86, CD163, and Arg I positive cells within the implants by using the optical brick technique, as described (9). Numerical density (N_V) estimation was performed with the aid of a BH2 Olympus light microscope (magnification 100 \times , N.A. 1.25), a Heidenhain microcator (ND 281A) attached to the z axis of the microscope stage, and Kinetic Imaging Stereology 5.0 software. An unbiased sampling frame (USF) was applied under software control to each uniformly and randomly selected image (field of view) and the microcator set to zero. Each section was focused through in the z axis in a continuous motion; cells in the first (0–5 μm) and last (20–25 μm) 5 μm of the 25 μm sections were not counted to avoid the “lost cap” effect (10), generating a disector height of 15 μm within which cells were counted (verified by the microcator). Positively stained cells for CD3, CD4, FoxP3, CD68, CCR7, CD86, CD163, and Arg I were counted provided they obeyed the rules of the USF and were within maximum focus within the 15- μm disector height. Approximately 10 fields of view per tissue section were sampled by using a uniform random sampling approach, resulting in an average of 40–50 fields of view per scaffold.

Numerical density estimates (N_V) were calculated by using the following formula:

$$N_V = \frac{\sum Q}{\sum P(A_f h)},$$

where ΣQ is the total number of immunopositive cells counted, ΣP is the total number of frames, A_f is the area of the unbiased sampling frame and h is the disector height.

T-Cell Proliferation Assays. Isolation of splenocytes. Spleens were harvested from the same Sprague–Dawley rats that were used in the above biocompatibility study to minimize animal wastage. In these cases, only native or decellularized muscle tissue from a single rabbit, and from one side, was implanted into each rat. The contralateral rabbit CAD muscle was used for the preparation of recall antigen. All surrounding fat and mesentery was excised from the spleen and splenocytes isolated by using a 40- μm cell strainer (Fisherbrand; Fisher Scientific UK) and the back end of a plunger from a 10-mL syringe. Splenocytes were collected in fresh, serum-free RPMI medium 1640 medium (Gibco). Cells

were centrifuged at $200 \times g$ for 10 min (MSE Harrier 15/80; Henderson Biomedical) to form a pellet. The supernatant was siphoned off, and an equivalent volume of ACK lysing buffer (Lonza) was added to the remaining pellet to lyse red cells. Cells were resuspended in serum-free medium. Live cell counts and viability were performed by Trypan blue exclusion (Invitrogen) by using a hemocytometer and light microscope. Cell counts were confirmed by using a Sysmex hematology analyzer (Sysmex UK). In all cases, viability was $\geq 95\%$. Splenocytes were also isolated from rabbit spleens for the two-way mixed lymphocyte reaction (MLR) controls.

Preparation of recall antigen. Because the rabbit CAD muscle is a paired muscle, one side was kept fresh, or decellularized, and implanted into Sprague–Dawley rats, from which the spleen was subsequently harvested and splenocytes isolated. The contralateral side was treated in exactly the same way (left fresh or decellularized) but was snap-frozen in isopentane (2-methylbutane; Sigma-Aldrich) precooled over liquid nitrogen and stored at -80°C until required. For coculture experiments, 5-mm punch biopsies of native, or decellularized, muscle tissue were taken (Stiefel Laboratories) and, following sterilization with ultraviolet light, were cocultured with labeled rat splenocytes.

Carboxyfluorescein diacetate succinimidyl ester assay. Carboxyfluorescein diacetate succinimidyl ester (CFSE; also known as CFDA-SE) is a nonradioactive, fluorescent intracellular dye that permanently marks cells and allows their fate to be followed. Cells suspended in serum-free RPMI medium 1640 (Gibco) were stained with CFSE dye (Molecular Probes) to give a final CFSE concentration of $1\ \mu\text{M}$. Cells were incubated at 37°C for 10 min. The reaction was quenched by diluting the cells/CFSE in 20–30 mL of RPMI medium 1640, supplemented with 10% FCS (South American origin; Lonza) and 1% penicillin-streptomycin (Gibco). Cells were centrifuged at $200 \times g$ for 10 min and washed three times in RPMI medium 1640, supplemented with 10% serum and 1% penicillin-streptomycin to remove excess, unbound CFSE dye. An aliquot of cells was removed for baseline staining to confirm desired staining had been achieved before incubation.

Cells were incubated in suspension culture at 1×10^6 cells per mL in nontissue culture treated 48- and 96-well plates (BD Biosciences) at 37°C , 5% CO_2 for 72 h in RPMI medium 1640, supplemented with 10% serum and 1% penicillin-streptomycin. All experiments were conducted in triplicate. A number of controls, in addition to the test conditions were required, as follows: (i) unstained rat splenocytes (CFSE negative cells) to quantify background fluorescence; (ii) unstimulated stained rat splenocytes (CFSE-positive cells cultured alone in medium)—negative control; (iii) stained rat splenocytes stimulated with $1\ \mu\text{g}/\text{mL}$ SEB—positive control; (iv) two-way MLR. For this experiment stained rat splenocytes were cocultured with unstained rabbit splenocytes to ensure that rat splenocytes responded appropriately by proliferating in response to rabbit antigens; and (v) test conditions consisting of stained splenocytes cocultured with native, or decellularized, muscle.

After incubation, cells were harvested and their viability were checked by taking off a small aliquot for Trypan blue exclusion. Viability was $\geq 95\%$ in all cases. Adherent cells to the scaffold and tissue were detached by washing the tissue and gentle trituration with a pipette. Cells were incubated with the monoclonal antibody, APC mouse IgM κ anti-rat CD3 (BD Biosciences), PE-Cy5 mouse IgG2a κ anti-rat CD4 (BD Biosciences), APC mouse IgG2a κ anti-rat CD8 (Biolegend), or an equivalent isotype-matched negative control antibody (BD Biosciences).

Samples were processed by using a BD FACScan machine (BD Biosciences), with Rainbow 4 and 5 color upgrade (Cytex Development), acquiring a minimum of 20,000 live events from each sample. Data were acquired by using BD CellQuest Pro software (version 4.0.1 for Mac; BD Biosciences) and analyzed by using FlowJo software (version 7.6.5; Tree Star). The gating strategy

used was debris exclusion and positive gating of the lymphocyte population on the forward scatter–side scatter dot plot. Out of the live cells, $\text{CD}3^+$, $\text{CD}4^+$, and $\text{CD}8^+$ cells were shown in a dot plot against CFSE and the percentage of proliferated cells was measured on a histogram, expressed here as the proliferation index (i.e., the proportion of cells that have proliferated one, or more, times in response to the antigenic stimulus). Supernatants were collected from the same cell suspensions and stored at -80°C for future cytokine analysis.

Cytokine Analysis (Cytometric Bead Array). Culture supernatants were analyzed by using the BD cytometric bead array rat flex sets (BD Biosciences) for IL-2, IL-10, IFN- γ and tumor necrosis factor- α . For this procedure, frozen supernatants were thawed and the manufacturers' protocols were followed by measuring the above cytokines in undiluted samples against the included standards. Data were acquired by flow cytometry as above and analysis was carried out by using FCAP Array software (BD Biosciences). Cytokine concentrations are expressed as picograms per milliliter per 1×10^6 cells per mL, cultured for 72 h under standard cell culture conditions (37°C , 5% CO_2 in RPMI medium 1640, supplemented with 10% serum and 1% penicillin-streptomycin).

Seeding Experiments in Vivo. Mouse-EYFP⁺ myoblast isolation and culture. Three month-old C57BL/6 mice ubiquitously expressing the enhanced yellow fluorescent protein under the control of the β -actin promoter were used in these experiments (11).

Single myofibers were isolated from the above animals, as described (12, 13). In brief, single muscle fibers with associated satellite cells (SCs) were isolated from the hindlimb skeletal muscles (extensor digitorum longus, flexor digitorum brevis, and soleus) following enzymatic digestion with 0.2% (wt/vol) type I collagenase (Sigma-Aldrich), reconstituted in Dulbecco's modified eagle medium (DMEM) low-glucose (Gibco) (supplemented with 1% penicillin-streptomycin; Gibco) for 2 h at 37°C . Following digestion, muscles were transferred to a 10-cm horse serum-coated plate (BD Biosciences) containing 10 mL of plating medium (primary dilution), composed of DMEM low-glucose, 10% horse serum (Gibco), 1% penicillin-streptomycin, 0.5% chicken embryo extract (CEE; Seralab), and gently triturated by using a wide-bore micropipette to release single myofibers. To minimize the contribution of nonmyogenic, contaminant cells (interstitial, hematopoietic, and endothelial cells), single fibers were carefully sucked up under an inverted phase contrast microscope (Zeiss AX10; Carl Zeiss) with a 200- μL pipette and serially transferred through two further 10-cm horse serum-coated dishes containing plating medium (secondary and tertiary dilutions).

Fibers were seeded on to 10-cm plates precoated with 10% Matrigel in DMEM (incubation for 1 h at 37°C ; BD Biosciences) and incubated at $37^\circ\text{C}/5\% \text{CO}_2$. Proliferation medium (DMEM low-glucose containing 20% FBS, 10% horse serum, 0.5% CEE, and 1% penicillin-streptomycin) was carefully added 24–48 h after seeding individual fibers and changed every 2–3 d. After SCs left their parental myofibers and started to proliferate, they were trypsinized at 70% confluence and expanded. Cells at passage two, or less, were used for transplantation experiments. Live cell counts and viability were performed by Trypan blue exclusion (Invitrogen) by using a hemocytometer. In all cases, viability was $\geq 95\%$ before seeding. The myogenicity of fiber-derived cells was confirmed by inducing their differentiation in fusion medium (DMEM low-glucose, 2% horse serum, 0.5% CEE, and 1% penicillin-streptomycin).

Preparation of decellularized scaffolds. Decellularized scaffolds were prepared as described above. Scaffolds were obtained from the tibialis anterior muscle of New Zealand White rabbits (Pneumolabs UK) and wild-type Sprague–Dawley rats (Charles River UK). Six-millimeter punch biopsies (Miltex) ensured standardization of scaffold size across experiments. Scaffolds were produced

fresh for each experiment and, following decellularization, were stored in 5% (vol/vol) antibiotic-antimycotic (Sigma-Aldrich) in PBS for no more than 2 d before cell seeding experiments, to minimize the risk of contamination. Before cell seeding experiments, scaffolds were sterilized under a UV lamp (30 min each side). Routine H&E staining was performed as a quality control on a piece of scaffold fixed in 10% NBF to confirm complete decellularization before cell seeding.

Coagulated polycaprolactone fabrication. Coagulated poly(ϵ -caprolactone) (PCL) was prepared by an extrusion-phase inversion method, similar to that described for POSS-PCU (polyhedral oligomeric silsesquioxane [POSS] covalently bonded to poly(carbonate-urea)urethane [PCU]) (14).

In brief, cast PCL was dissolved in dimethylacetamide (Sigma-Aldrich) to a final concentration of 25% (wt/vol) and heated at 60 °C for 15 min in an ultrasonic bath sonicator to form a viscous gel. To induce porosity, 40- μ m sodium bicarbonate particles (pre-sieved in a 300- μ m sieve; Brunner Mond UK) were added to the resulting mixture to a final porogen concentration of 40% (wt/vol), together with 2% (vol/vol) Tween-20 (Sigma-Aldrich). The resulting mixture was left to degas for 10 min at room temperature and then poured into a custom-made mold to create a sheet of coagulated PCL 5 mm thick. The mold was carefully placed into reverse osmosis water, and the water changed daily for 4 d to clear dimethylacetamide and permit salt particulate leaching.

Coagulated PCL was stored in 5% (vol/vol) antibiotic-antimycotic (Sigma-Aldrich) in reverse osmosis water. Before cell seeding experiments, PCL scaffolds were sterilized under a UV lamp (30 min each side). Scaffold size was standardized across experiments through the use of 6.0-mm punch biopsies (Miltex).

Preparation of seeded scaffolds. Tissue-engineered constructs were prepared by statically seeding EYFP-mouse myoblasts on to pre-sterilized decellularized rabbit, rat, and coagulated PCL scaffolds in 24-well plates (Corning), at a seeding density of 5×10^5 cells per scaffold. Cells were injected with a 26 gauge, 3/8-inch needle on a 1-mL syringe (BD Medical) into four separate places within each scaffold, within a total cell suspension volume of 20 μ L per scaffold in proliferation medium. Seeded scaffolds were incubated at 37 °C, 5% CO₂. Two hours after incubation, 100 μ L of warm (37 °C) proliferation medium was added to each scaffold before returning them to the incubator. Before transplantation, seeded

scaffolds were fixed in 4% glutaraldehyde for scanning electron microscopy (SEM) analysis.

Surgical procedure. Thirty-eight adult male Sprague–Dawley rats (Charles River UK), weighing 250–400 g, were anesthetized as described above (biocompatibility study). Under aseptic technique and after shaving the left hindlimb fur, the skin of one of the hindlimbs was incised longitudinally under gentle tension and the tibialis anterior (TA) muscle was exposed. Muscle fibers were separated gently, and an equivalent wedge of tissue was removed from the core of the TA muscle on one side, to create a volumetric muscle loss. The contralateral limb was left intact, thereby serving as an internal control. Consistency of the injury between animals was ensured by using a 4.0-mm punch biopsy (Mediatech Systems) and weighing the excised tissue with a microbalance (A&D Company) to assess the repeatability of the ablation.

The defect created in the core of the TA muscle by the 4.0-mm punch biopsy was replaced with the respective tissue-engineered construct (6.0-mm scaffold together with the donor-labeled cells). Following transplantation, the fascia overlying the TA muscle was sutured and the overlying skin closed.

No animals received immunosuppressive treatment. At 2 and 4 wk, rats were humanely euthanized by anesthetic overdose at which point the explants were harvested and processed for histology and immunohistochemistry. The primary morphological outcome was donor cell survival, as determined by EYFP analysis. The number of cells in the respective implants were quantified by two independent, blinded investigators by determining the number of EYFP⁺ cells per random high power field on merged images of EYFP/DAPI (40 \times magnification).

Statistical Analysis. Data were calculated as mean \pm SD, unless otherwise stated. Significance was determined by performing one-way or two-way analysis of variance (ANOVA) with Tukey–Kramer multiple comparison post tests (for comparisons across more than two groups), two-tailed unpaired Student *t* tests (for parametric data, where comparing data between two groups) or Mann–Whitney tests (for nonparametric data, where comparing data between two groups). Statistical analysis was performed by using SPSS Statistics 20 (SPSS Inc.) and GraphPad Prism 6 (GraphPad Software). A *P* value of less than 0.05 was considered to be significant.

1. Fishman JM, Ansari T, Sibbons P, De Coppi P, Birchall MA (2012) Decellularized rabbit cricoarytenoid dorsalis muscle for laryngeal regeneration. *Ann Otol Rhinol Laryngol* 121(2):129–138.
2. Gillies AR, Smith LR, Lieber RL, Varghese S (2011) Method for decellularizing skeletal muscle without detergents or proteolytic enzymes. *Tissue Eng Part C Methods* 17(4):383–389.
3. Granzier HL, Irving TC (1995) Passive tension in cardiac muscle: Contribution of collagen, titin, microtubules, and intermediate filaments. *Biophys J* 68(3):1027–1044.
4. Totonelli G, et al. (2012) A rat decellularized small bowel scaffold that preserves villus-crypt architecture for intestinal regeneration. *Biomaterials* 33(12):3401–3410.
5. Baiguera S, et al. (2011) Development of bioengineered human larynx. *Biomaterials* 32(19):4433–4442.
6. Baiguera S, et al. (2010) Tissue engineered human tracheas for in vivo implantation. *Biomaterials* 31(34):8931–8938.
7. Mayhew TM (1991) The new stereological methods for interpreting functional morphology from slices of cells and organs. *Exp Physiol* 76(5):639–665.
8. Gerhardt LC, et al. (2011) The pro-angiogenic properties of multi-functional bioactive glass composite scaffolds. *Biomaterials* 32(17):4096–4108.
9. Widdows K, Kingdom JC, Ansari T (2009) Double immuno-labelling of proliferating villous cytotrophoblasts in thick paraffin sections: Integrating immuno-histochemistry and stereology in the human placenta. *Placenta* 30(8):735–738.
10. Howard V, Reid S, Baddeley A, Boyde A (1985) Unbiased estimation of particle density in the tandem scanning reflected light microscope. *J Microsc* 138(Pt 2):203–212.
11. Srinivas S, et al. (2001) Cre reporter strains produced by targeted insertion of EYFP and ECFP into the ROSA26 locus. *BMC Dev Biol* 1:4.
12. Urbani L, Piccoli M, Franzin C, Pozzobon M, De Coppi P (2012) Hypoxia increases mouse satellite cell clone proliferation maintaining both in vitro and in vivo heterogeneity and myogenic potential. *PLoS ONE* 7(11):e49860.
13. Rossi CA, et al. (2011) In vivo tissue engineering of functional skeletal muscle by freshly isolated satellite cells embedded in a photopolymerizable hydrogel. *FASEB J* 25(7):2296–2304.
14. Jungebluth P, et al. (2011) Tracheobronchial transplantation with a stem-cell-seeded bioartificial nanocomposite: A proof-of-concept study. *Lancet* 378(9808):1997–2004.

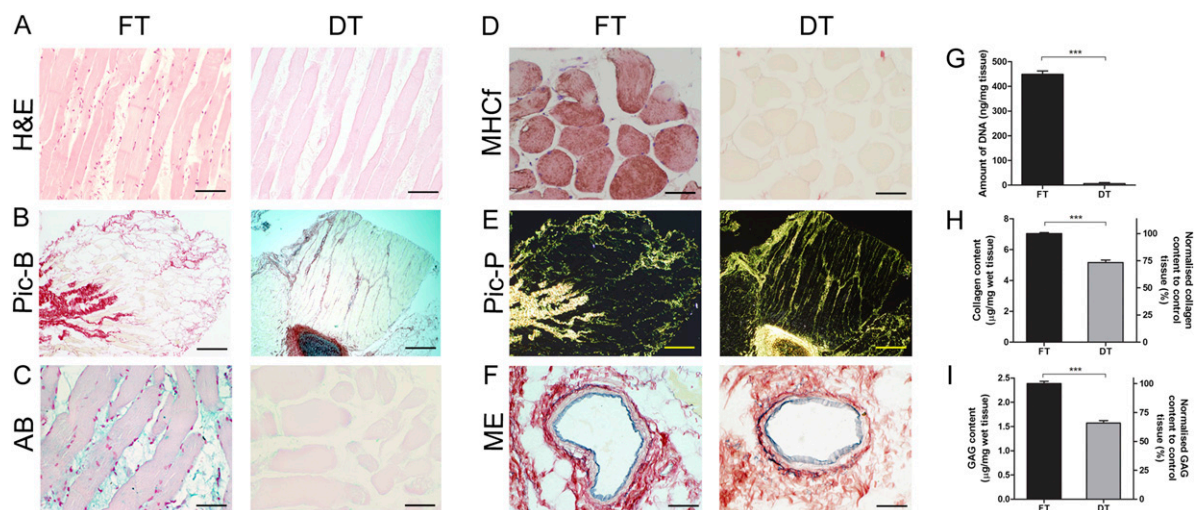


Fig. S1. Characterization of a decellularized skeletal muscle scaffold for tissue engineering. (A) H&E staining demonstrating loss of nuclei and preservation of morphology in decellularized tissue (DT) compared with fresh tissue (FT). Collagen staining with Picrosirius-red stain under brightfield microscopy (B) and plane polarized light (E) of FT and DT, respectively. Glycosaminoglycan (GAG) staining with Alcian blue (C) and elastin staining with Miller's elastin (F). (D) Immunohistochemistry of myosin heavy chain (fast fibers). (G) DNA quantification. (H) Collagen quantification. (I) Sulfated-GAGs quantification of FT and DT, respectively. (Scale bars: A, 100 µm; C, D, and F, 50 µm; B and E, 500 µm.) $n = 12$ in each group. Statistical significance is indicated by the asterisks where $***P < 0.001$.

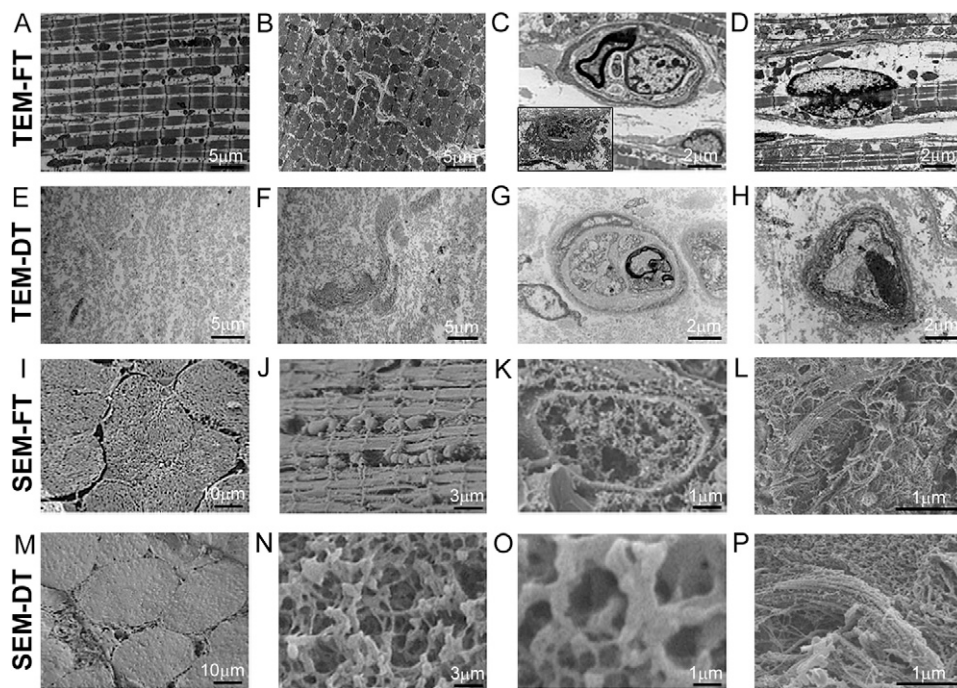


Fig. S2. Transmission electron microscopy (TEM) (A–H) and scanning electron microscopy (SEM) (I–P) of FT and DT, respectively. DT results in loss of the actin-myosin filaments and nuclei (E and N) compared with FT (A–D and I–L), with preservation of overall muscle fiber morphology (M) and collagen fibers in DT (F and P). Decellularized axonal and blood vessel structures are seen in DT (G and H). C Inset represents a neuromuscular junction seen at higher power magnification in FT. Decellularization leads to the generation of a porous matrix (N and O). Scale bars as shown in the figure.

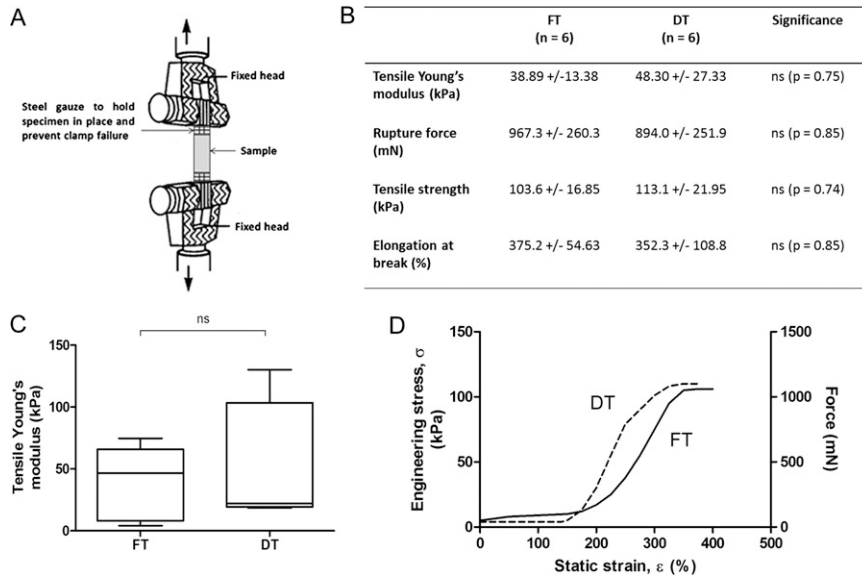


Fig. S3. Biomechanical assessment of FT and DT, respectively. (A) Experimental setup for measuring biomechanical parameters as shown in B and C. Comparable biomechanical properties were seen between DT and FT (B and C). (D) Tensile stress–strain relationships of FT and DT. $n = 6$ in each group. Statistical significance is indicated by the asterisks where ns = not significant.

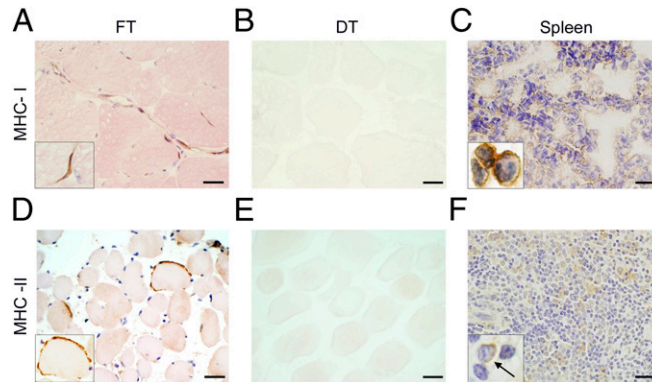


Fig. S4. MHC-I (A–C) and MHC-II (D–F) immunohistochemistry for FT (A and D) and DT (B and E), respectively. Decellularization led to loss of MHC-I from endothelial cells lining blood vessels (B) compared with FT (A) and MHC-II from the surface of muscle fibers (E) compared with FT (D). Spleen was used as a positive control for MHC-I (C) and MHC-II (F). Insets taken at higher power magnification. (Scale bars: 50 μm .)

